Journal of Applied Polymer Science

Structural and Dielectric Studies of Amorphous and Semicrystalline Polymers Blend-Based Nanocomposite Electrolytes

Shobhna Choudhary, Ram Jeewan Sengwa
Department of Physics, Dielectric Research Laboratory, Jai Narain Vyas University, Jodhpur 342 005, India
Correspondence to: S. Choudhary (E-mail: shobhnachoudhary@rediffmail.com)

ABSTRACT: The solid polymeric nanocomposite electrolyte (SPNE) films based on the blend of amorphous poly(methyl methacrylate) (PMMA) and semicrystalline poly(ethylene oxide) (PEO) (PMMA:PEO = 80:20 wt %) doped with lithium perchlorate ($LiClO_4$) salt and montmorillonite (MMT) clay nanofiller were prepared by classical solution cast, ultrasonic assisted solution cast and ultrasonication along with microwave irradiated solution cast followed by melt-pressing methods. The X-ray diffraction study of these electrolytes revealed the amorphous behavior with intercalated MMT structures. The suppressed crystallinity of PEO in the blend electrolyte complexes confirmed the existence of single discrete PEO chains confined within the PMMA domains. The dielectric relaxation spectroscopy of these materials was performed over the frequency range 20 Hz to 1 MHz, at ambient temperature. The presence of a singular relaxation peak in the loss tangent and electric modulus spectra of these electrolytes confirms a coupled cooperative chain segmental dynamics of the blend polymer owing to their miscible amorphous morphology. The behavior of transient complexes formed between the polymers functional groups, lithium cations and the intercalated MMT nanoplatelets was explored. The ambient temperature ionic conductivity of these electrolytes depends on the structural dynamics and the sample preparation methods. It is revealed that the presence of PEO in the PMMA matrix mainly governs the structural, dielectric, and ionic properties of these SPNE films. © 2014 Wiley Periodicals, Inc. J. Appl. Polym. Sci. **2015**, *132*, 41311.

KEYWORDS: batteries and fuel cells; blends; clay; dielectric properties; X-ray

Received 18 April 2014; accepted 21 July 2014
DOI: 10.1002/app.41311

INTRODUCTION

In the last one decade, the solid polymeric electrolytes (SPEs) have been a topic of great technological interests because of their uses in the high power and high energy density storage lithium-ion batteries.[1–44] These batteries are the promising power sources for the modern portable electronic equipments and the electrical vehicles. In addition to the batteries, the SPEs are also used in fabrication of various ion conducting electrochromic devices.[13,15] The main characteristics of the SPEs are their light weight, leak proof, flexible and compact in size and longer life span with improved safety and electrochromical performances, which make them superior over the liquid and ceramic electrolytes. Poly(ethylene oxide) (PEO)[1–4,6–12] and poly(methyl methacrylate) (PMMA)[5,20–22,35–44] are better considerations among the polymers host for preparation of the SPE materials. Owing to the environmental friendly, high solvating power in the solid state for alkali metal salts and highly flexible type film forming ability of the PEO, it has become the first choice of the investigators for preparation of SPEs both by the solution–cast as well as melt compounding methods. The only disadvantage of PEO is its semicrystalline structure, which results the low ionic conductivity of the SPEs based on it, at ambient temperature. Because in regards to the SPEs, it has been established that the effective ion transport can be the best achieved in an amorphous phase of the host polymer.[22] On the other hand, PMMA is an amorphous, light weight and transparent polymer, and it has highly active electron donating carbonyl (C=O) functional group for the cations coordination of the alkali metal salts.[5,20–22] But the electrolyte film based on PMMA matrix is always found highly brittle in nature which restricts its suitability for the fabrication of different shapes and flexible type ion conducting devices.

For better ion conducting performances along with the tailor-made physico-chemical properties of the PMMA and PEO-based electrolytes, the investigators adopted several strategies, viz. different methods of preparation[1–5,7,9,10,12,19] (solution–cast, melt compounding, ultrasonic assisted, microwave irradiated, ion irradiated methods, etc.), addition of liquid plasticizers,[4,15,23,26,30,37] dispersion of inorganic nanofillers,[9–12,21,23–29,32–36,38] use of different salts,[1,5–7,20,22,27,30] and their blending with other polymers.[17,22,39–44] These studies revealed that the addition of plasticizers always increased the degree of salt dissociation and the amorphous phase

of the SPE materials, which resulted in the increase of their ionic conductivity. But the mechanical, thermal and dimensional stability of the plasticized solid polymer electrolytes (PSPEs) are adversely affected as compared to the electrolytes having no plasticizer. On the other hand, the dispersion of inorganic nanofillers significantly improves the physico-chemical properties, and simultaneously increases the amorphous phase which is needed to enhance the ionic conductivity of the solid polymer nanocomposite electrolytes (SPNEs).

In the last several years, the preparation and studies established that the blending of PMMA and PEO is an effective and economic way of creating high performance material to overcome the drawbacks of the individual polymer.[45–53] The blending of a small amount of PEO in the PMMA matrix results in a large increase of PMMA flexibility and reduces its brittleness, and simultaneously the PMMA environment increases the amorphous phase of semicrystalline PEO. These tailored physico-chemical properties recognized the PMMA–PEO blend as a new novel material for the preparation of SPEs.[22,39,41,42,54,55] Recently,[22] the PMMA–PEO blend (50:50 wt %) with varying concentration of $LiClO_4$ has been studied in order to confirm their structural and ion conduction behavior with temperature variation. This study revealed that the increased amorphous phase of the electrolyte enhances the ionic conductivity, but it significantly reduces at high salt concentration due to the ion-pairing effect.

In this article, the PMMA–PEO blend matrix with lithium perchlorate ($LiClO_4$) as ion conducting salt and montmorillonite (MMT) clay as inorganic nanofiller has been used for the preparation of SPNE materials through different processing methods. It is well established that the dispersions of nano-meter sized MMT clay platelets (lamellar layered silicate) in the PEO matrix (PEO–MMT nanocomposites),[56–58] and also in the PMMA matrix (PMMA–MMT nanocomposites)[59–61] increase their mechanical, thermal, gas barrier, corrosion protection, UV resistance and nonflammable properties. Therefore, the consideration of MMT layered sheets as inorganic nanofiller in the PMMA–PEO blend is reasonable in the present study. Further, the MMT filled PEO-based SPNEs[11,12,19,25–29,62] and the MMT filled PMMA-based SPNEs[5,21,35,36] are gaining a lot of interest from both the technological and academic point of view. Mostly, the electrochemical properties of these SPEs and SPNEs are investigated by the impedance spectroscopy. The detailed dielectric properties and relaxation behavior of such materials are rarely explored using dielectric relaxation spectroscopy (DRS). Although, the dielectric properties of the electrolytes have the technological importance in fabrication of the ion conducting devices.[3,5–7] The knowledge of the ionic polarization and molecular relaxation mechanism of the composite system is a prerequisite for their successful applications. The study on (PMMA–PEO)–$LiClO_4$–MMT nanocomposite electrolytes having a very low concentration of the salt with varying composition of PEO in the PMMA matrix infers that the ionic conductivity of such materials is influenced by the MMT concentration and also the blend composition.[22,54,55]

Considering all the above mentioned facts on the polymeric electrolytes, in the present study (PMMA–PEO)–$LiClO_4$–x wt % MMT electrolyte films ($x = 0$–10) were prepared by three different processing methods, viz. "classical" solution cast melt-pressed, ultrasonicated solution cast melt-pressed and the ultrasonication along with microwave irradiated solution cast melt-pressed. The aims of this study are, firstly to explore the effects of material preparation methods on the dielectric properties, ionic conductivity and the molecular relaxations in the polymer blend-based complexed SPNE films. The comparative dielectric and electrical parameters of the samples prepared by three different methods are analyzed in order to confirm the most effective method of sample preparation for the enhancement of ionic conductivity of PMMA–PEO blend-based electrolytes. Secondly, it is intended to confirm the effect of MMT concentration on the dielectric properties and ionic conductivity of low salt concentration SPNE materials. Thirdly, it is aimed to reveal the intercalated/exfoliated MMT structures in these electrolytes using X-ray diffraction (XRD) measurements. Finally, an attempt is also made to explore the correlation between MMT structures, dielectric relaxation and ionic conductivity of the PMMA–PEO blend-based SPNE materials, which is so far to our best knowledge, has not been studied.

EXPERIMENTAL

Sample Preparation

PMMA ($M_w = 3.5 \times 10^5$ g mol^{-1}), PEO ($M_w = 6 \times 10^5$ g mol^{-1}), $LiClO_4$ (battery grade, dry, 99.9% metal basis), sodium-montmorillonite (MMT) clay (Nanoclay, PGV, a product of Nanocor®) and acetonitrile were obtained from Sigma-Aldrich. All the chemicals were vacuum dried at the standard temperatures before their use in preparation of the electrolytes. For the preparation of (PMMA–PEO)–$LiClO_4$–x wt % MMT films, the 80 : 20 wt % ratio of PMMA:PEO in the blend was used. The average molar ratio of [(C=O)+EO] : Li^+ = 15:1 was used for the electrolytes, where C=O is the carbonyl group of PMMA monomer unit, EO is the ether oxygen of PEO monomer unit and Li^+ is the lithium cation concentration in the electrolytes. The salt concentration is kept low for the preparation of these electrolytes in order to avoid the ion-pairing effect, which usually occurs at high concentration of the salt in polymer matrix. The required amounts of MMT for $x = 0$, 1, 3, 5, and 10 wt % with respect to the weight of PMMA–PEO blend were added as nanofiller for the preparation of the polymer blend-based nanocomposite electrolytes.

Three different processing methods as described below were used for the preparation of (PMMA–PEO)–$LiClO_4$–x wt % MMT electrolyte films.

1. "Classical" solution casting (SC) method: Initially, the polymeric electrolyte solutions consisted of the required amounts of PMMA, PEO, $LiClO_4$, and MMT for different MMT, concentrations were prepared in acetonitrile solvent in the separate glass bottles. These solutions were blended using magnetic stirrer to achieve the homogenous solution of each MMT concentration sample. After that they were cast onto Teflon petri dishes and by slow evaporation of solvent at

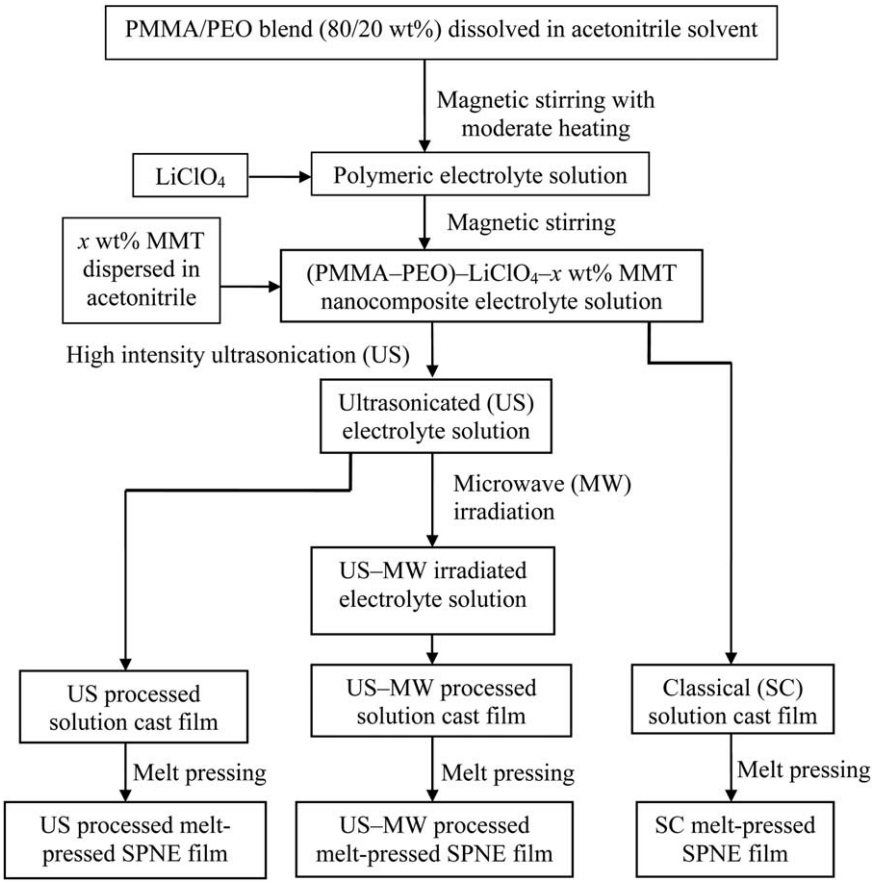

Scheme 1. Schematic illustration of different steps followed during the preparation of (PMMA–PEO)–$LiClO_4$–x wt % MMT nanocomposite electrolyte films by SC, US, and US–MW methods.

room temperature, the solution cast (SC) prepared (PMMA–PEO)–$LiClO_4$–x wt % MMT films were achieved.

2. Ultrasonic (US) processed solution casting method: In this method, initially the polymeric electrolyte solutions of different MMT concentrations were prepared as discussed above. After that each electrolyte solution was sonicated by ultrasonicator (250 W power, 25 kHz frequency) for 10 min duration with ON-OFF step of 15 s. In this processing the stainless steel sonotrode was directly immersed into the electrolyte solution for strong dose of the ultrasound. These ultrasonicated electrolyte solutions were cast to make the US processed prepared electrolyte films.
3. Ultrasonicated followed by microwave irradiation (US–MW) processed solution casting method: In this processing, firstly the ultrasonicated electrolyte solutions were prepared as mentioned above, and subsequently these solutions were irradiated by microwave energy using domestic microwave oven (600 W power and 2.45 GHz frequency) for 2 min duration of 10 s irradiation step with intermediate cooling. After that these US and MW irradiated electrolyte solutions were cast to obtain free standing US–MW processed prepared (PMMA–PEO)–$LiClO_4$–x wt % MMT electrolyte films.

These electrolyte films prepared by different methods were vacuum dried at 40°C for 24 h. After that each film was melted at 130°C in polymer film making unit and pressed under 2 tons of pressure per unit area. Cooling the material slowly up to room temperature, the smooth surfaces SPNE films were obtained for their dielectric and structural characterizations. The details of various steps followed during the processing of polymeric electrolyte solutions in different methods and the preparation of their films are depicted in Scheme 1.

Characterizations

The X-ray diffraction (XRD) patterns of the SPNE films and their constituents were recorded in reflection mode using a PANalytical X′pert Pro MPD diffractometer of Cu-Kα radiation (1.5406 Å) operated at 45 kV and 40 mA with a scanned step size of 0.05°/s. The powder samples of $LiClO_4$ and MMT were tightly filled in the sample holder, whereas the pristine PMMA, PEO and the SPNE films were placed on the top of the sample holder during their XRD measurements in the 2θ range 3.8–30°, at room temperature.

The dielectric and electrical spectra of the SPNE films were carried out using an Agilent technologies 4284A precision LCR meter and 16451B solid dielectric test fixture over the linear frequency f range from 20 Hz to 1 MHz, at ambient temperature (27 ± 1°C). Frequency dependent values of parallel capacitance C_p, parallel resistance R_p and loss tangent ($\tan\delta = \varepsilon''/\varepsilon'$) of the SPNE films were measured for the evaluation of their dielectric/

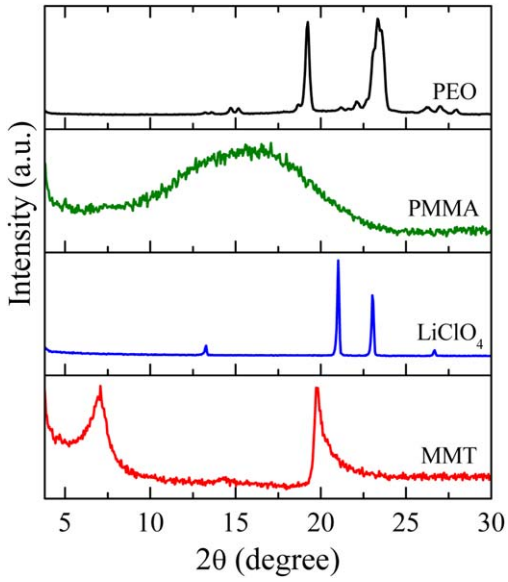

Figure 1. The XRD patterns of pristine PEO and PMMA films, and the $LiClO_4$ and MMT powder samples. [Color figure can be viewed in the online issue, which is available at wileyonlinelibrary.com.]

electrical spectra. Prior to samples measurement, the open circuit calibration of the cell was performed to eliminate the effect of stray capacitance of the cell leads. The spectra of intensive quantities, namely complex dielectric function $\varepsilon^*(\omega) = \varepsilon' - j\varepsilon''$, real part of alternating current (ac) electrical conductivity $\sigma' = \omega\varepsilon_0\varepsilon''$ and electric modulus $M^*(\omega) = M' + jM''$, and the extensive quantity i.e. complex impedance $Z^*(\omega) = Z' - jZ''$ of the SPNE films were determined using the expressions described in detail elsewhere.[5,63,64]

RESULTS AND DISCUSSION

Structural Analysis

The XRD patterns of $LiClO_4$, MMT, PEO, and PMMA over the angular range 3.8–30° are shown in Figure 1, which are in agreement with their earlier reported patterns.[5,20,65] The $LiClO_4$ has major crystalline peaks at $2\theta = 21.02°$ and 23.04°,[20] whereas the MMT has reflection peaks at $2\theta = 7.03°$ and 19.79° which are corresponding to its 001 and 101 reflection planes.[65] The pure PEO has major crystalline peaks at $2\theta = 19.22°$ and 23.41° corresponding to the crystal reflections 120 and concerted 112,032 planes which reveal its semicrystalline behavior.[7,19,65] The observed broad and diffused peak around 16° of pure PMMA confirms its predominantly amorphous phase.[5,20]

Figure 2(a–c) shows the XRD patterns of (PMMA–PEO)–$LiClO_4$–x wt % MMT films prepared by SC, US, and US–MW methods. The crystalline peaks of $LiClO_4$ and PEO are not found in the XRD patterns of these electrolytes, which infer that the added $LiClO_4$ amount is completely dissociated into cations Li^+ and anions ClO_4^-, and the crystallinity of blended PEO with the PMMA matrix is fully suppressed. In these electrolytes the salt dissociation occurs due to ion-dipolar coordination formed between the functional groups of the polymers and the cations of salt. From these observations, it can be concluded that the 80/20 wt % blend of PMMA/PEO forms the complete miscible complexed structures of single discrete PEO chain confined within the PMMA domains, which are in consistent with earlier results.[45–48,55] In case of PEO–$LiClO_4$ electrolytes,[10] the crystallinity of PEO decreased due to its complexes with Li^+ but the materials is not changed completely into an amorphous structure, as observed for these PMMA–PEO blend-based electrolytes. Further, the PMMA-based PMMA–$LiClO_4$–x wt % MMT electrolytes of MMT low concentration have complete amorphous behavior with exfoliated MMT structures.[5]

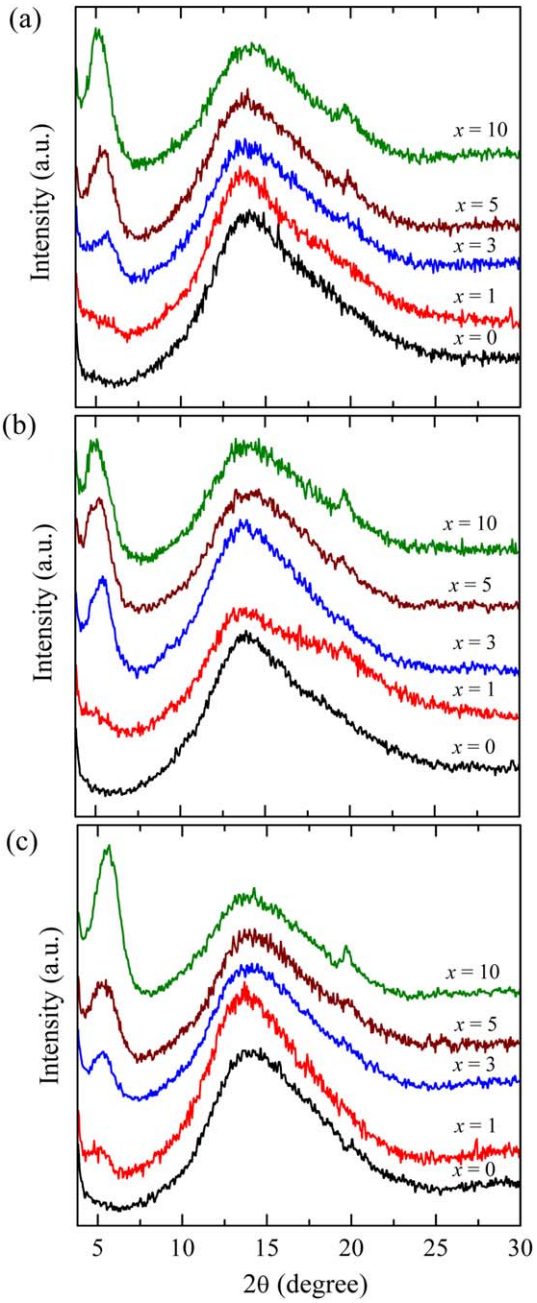

Figure 2. The XRD patterns of (PMMA–PEO)–$LiClO_4$–x wt % MMT nanocomposite electrolyte films prepared by (a) SC, (b) US, and (c) US–MW methods. [Color figure can be viewed in the online issue, which is available at wileyonlinelibrary.com.]

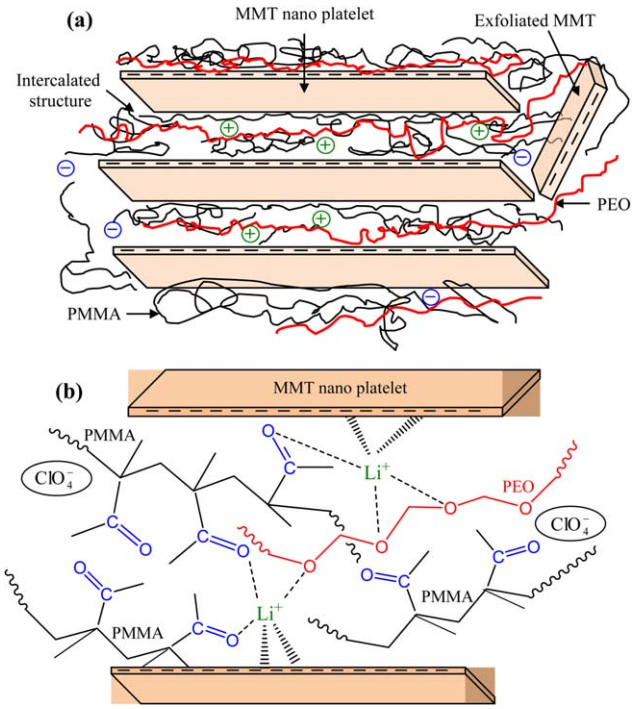

Scheme 2. Schematic representation of; (a) intercalated and exfoliated MMT structures, and (b) ion-dipolar and ion-ion interactions in cations coordinated polymers blend intercalated MMT structure in the (PMMA–PEO)–$LiClO_4$–*x* wt % MMT nanocomposite electrolyte film. [Color figure can be viewed in the online issue, which is available at wileyonlinelibrary.com.]

The XRD patterns of these MMT filled electrolyte films (except 1 wt % SC and US processed prepared films) have 001 reflection peaks of MMT in the range 5 to 6° which are at lower angle side as compared to the peak position 7.03° of pristine MMT. These 001 peaks positions confirm the formation of intercalated MMT structures in the PMMA–PEO blend-based nanocomposite electrolytes. From the intercalated structural behavior of PEO–MMT nanocomposite[65] and the exfoliated MMT structures of PMMA–$LiClO_4$–*x* wt % MMT electrolytes,[5] it can be concluded that the formation of intercalated MMT structures in these PMMA–PEO blend-based electrolytes is due to the presence of PEO in the composite. The values of *d*-spacing corresponding to 001 crystalline peak d_{001} are determined by the Bragg's relation $\lambda = 2d\sin\theta$, where λ is the wavelength of X-ray radiation ($\lambda = 1.5406$ Å), *d* is the spacing between diffractional lattice planes and θ is the diffraction angle of the peak. The values of d_{001} of these electrolytes are found in the range 1.56–1.77 nm which vary with the MMT concentration and also the sample preparation methods.

In the formation of intercalated nanocomposites, the galleries of MMT layers are occupied by the polymeric structures.[14,65] The intercalation occurs mainly due to favorable interactions compatibility between the functional group of polymer and the surface charge of MMT nanoplatelets. Scheme 2 shows the schematic representation of the nanocomposites formed due to the intercalation of PMMA–PEO blend complexes into the MMT galleries. The first one structure [Scheme 2(a)] shows that the complexes of PEO molecules confined within PMMA domain enter between the MMT platelets and increase the clay gallery spacings (d_{001}), which result in the intercalated nanocomposites. But the adsorption of polymers on the MMT surfaces also delaminates (exfoliates) the MMT nanoplatelets and form the exfoliated nanocomposites. The Lewis acid-base interactions of the polymers/Li^+/MMT in these nanocomposites are depicted in Scheme 2(b). The Li^+ has four to six sites of coordination with the electron donating groups of polymers and also the negatively charged MMT nanoplatelets.[5,21,25,28,29] Due to the EO···Li^+, C=O···Li^+, MMT···Li^+, and C=O···Li^+···EO types of possible interactions can result in a variety of transient complexes of these nanocomposites. In these complexes, the anions ClO_4^- mostly remain un-coordinated somewhere in the polymer backbone as shown in Scheme 2(b). In these materials, the Li^+···MMT interactions also facilitate the intercalation of polymer–cations complexes into the MMT galleries, but the material preparation processing methods alter the intercalated amount of the polymers blend. The exfoliated MMT nanosheets no longer display the 001 reflection peak,[5] and therefore the 1 wt % MMT filled SC and US processed prepared electrolytes have completely exfoliated MMT structures, whereas the US–MW processed prepared electrolyte film of 1 wt % MMT concentration has some amount of intercalated structures beside the exfoliation.

Figure 2(a–c) shows that the intensity values of 001 peak have an increase with the increase of MMT concentration for the SC and US–MW processed prepared electrolyte films, but these values are found nearly same for the US processed prepared electrolytes having 3 to 10 wt % MMT. The comparative peak intensities infer that the amount of intercalated polymers blend significantly varies with the change of MMT concentration and also with the samples preparation methods. The values of MMT clay gallery width W_{cg} of these SPNE films is determined by the relation $W_{cg} = d_{001} - W_{cl}$, where W_{cl} is the MMT clay layer width in *c*-axis, which is 0.96 nm.[11] The d_{001} spacing value for the MMT powder is 1.257 nm and its W_{cg} value is found 0.297 nm. The observed W_{cg} values of the electrolytes (range from ~0.6 to 0.8 nm) reveal that the intercalated complexes of PMMA–PEO blend have the flattened-type morphological arrangements in the swelled MMT galleries, because the trans conformation of PEO chain increases the MMT gallery expansion of about 0.4 nm.[65,66]

Dielectric Behavior

The real part of complex permittivity ε' and dielectric loss ε'' spectra of (PMMA–PEO)–$LiClO_4$–*x* wt % MMT electrolytes prepared through SC, US and US–MW methods are shown in Figure 3(a–c). The ε' values of these electrolytes have decrease with increase of frequency and finally attain the steady state near 1 MHz, which are corresponding to the high frequency limiting permittivity ε_∞ values.[5–7] These ε_∞ values of the investigated electrolytes are found in the range ~2 to 4. A close look on the ε' spectra reveals that the frequency dependent ε' values of an electrolyte film significantly vary with the sample preparation methods and also with the concentration of MMT nanofiller. Comparatively less variations in ε' values with change of MMT concentration of the US–MW processed prepared electrolyte films infer that similar type of dipolar ordering are formed

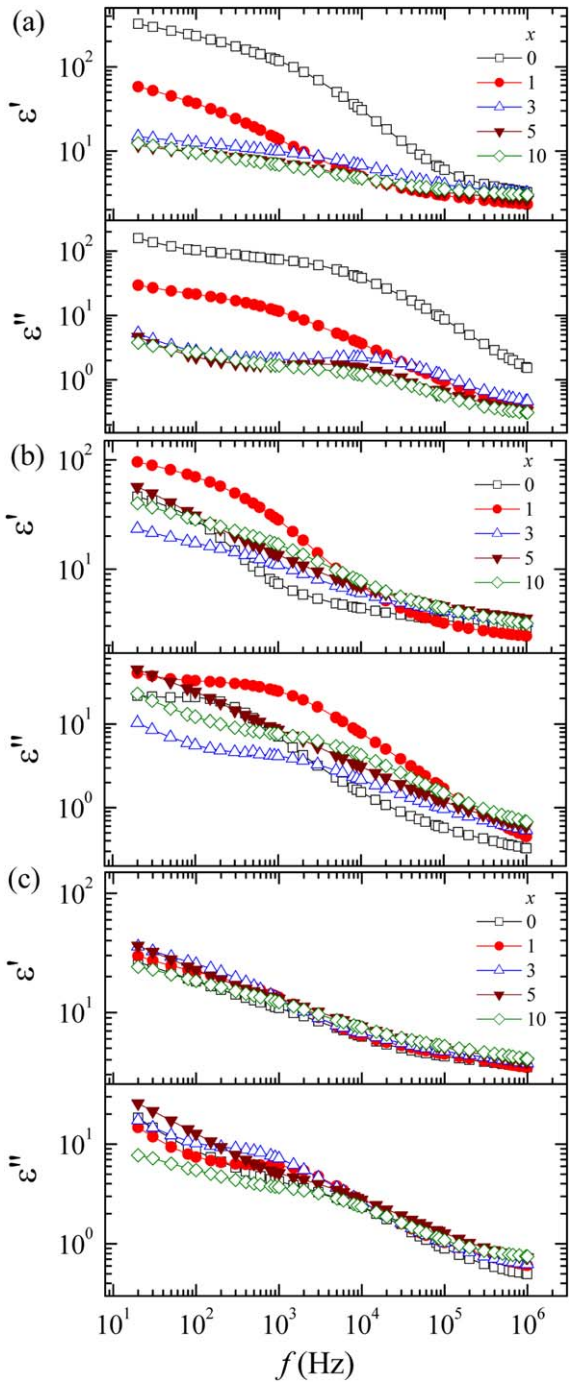

Figure 3. Frequency dependent real part ε' and loss ε'' of the complex dielectric function of (PMMA–PEO)–$LiClO_4$–x wt % MMT nanocomposite electrolyte films prepared by (a) SC, (b) US, and (c) US–MW methods. [Color figure can be viewed in the online issue, which is available at wileyonlinelibrary.com.]

due to microwave irradiation, which are not the case of SC and US assisted prepared electrolyte films. Further, the anomalous behavior of the ε' values with increase of MMT concentration suggests the existence of randomly oriented exfoliated MMT nanoplatelets in the polymer blend matrix which alters the total dielectric polarization. Some samples have relatively high ε' values at low frequencies, which is owing to the contribution of electrode polarization (EP) effect.[5–7,19,27–29] The low frequency ε' values of PEO–$LiClO_4$ and PEO–$LiClO_4$–x wt % MMT electrolytes[6,7,10] were found of the order of 10^3-10^5, whereas PMMA–$LiClO_4$ and PMMA–$LiClO_4$–x wt % MMT electrolytes[5] had the ε' values only of one order of magnitude. But the

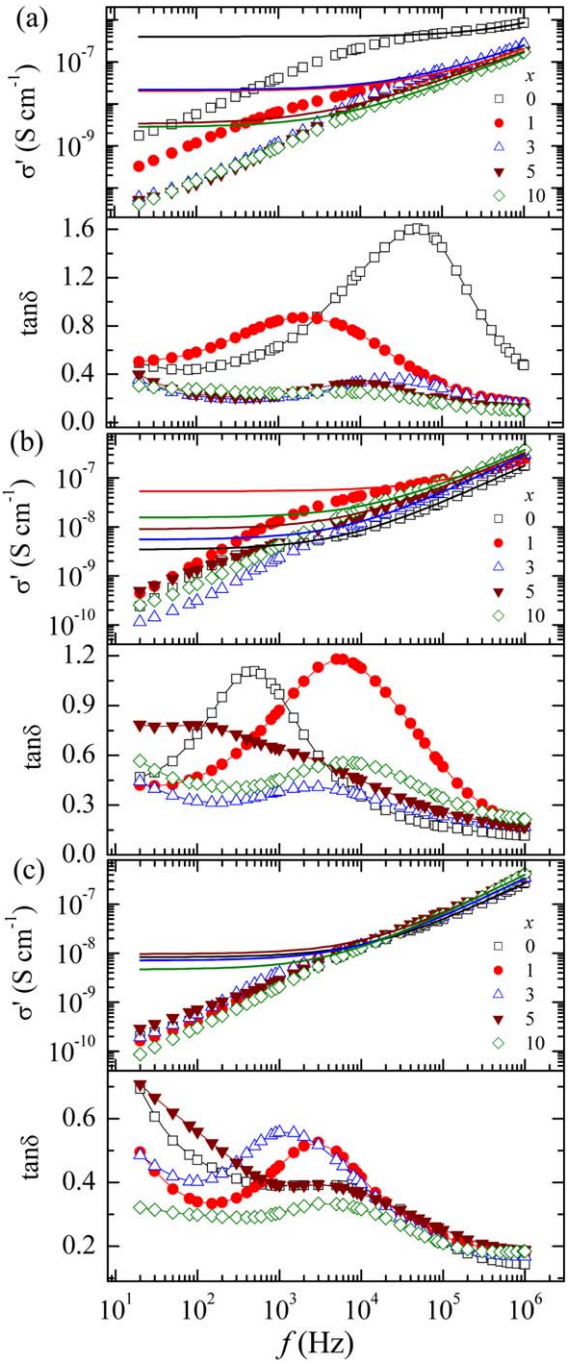

Figure 4. Frequency dependent real part of ac conductivity σ' and loss tangent (tanδ) of (PMMA–PEO)–$LiClO_4$–x wt % MMT nanocomposite electrolyte films prepared by (a) SC, (b) US, and (c) US–MW methods. The continuous solid lines in σ' spectra represent the fit of experimental data to the Jonscher power law $\sigma'(\omega) = \sigma_{dc} + A\omega^n$. [Color figure can be viewed in the online issue, which is available at wileyonlinelibrary.com.]

Table I. Values of Loss Tangent Relaxation Time $\tau_{\tan\delta}$, Electric Modulus Relaxation Time τ_M, dc Ionic Conductivity σ_{dc} and Fractional Exponent n of (PMMA–PEO)–$LiClO_4$–x wt % MMT Nanocomposite Electrolyte Films Prepared by SC, US, and US–MW Methods

x wt % MMT	$\tau_{\tan\delta}$ (μs)	τ_M (μs)	$\sigma_{dc} \times 10^7$ (S cm^{-1})	n
Classical SC prepared SPNE films				
0	3.25	0.33	3.98	0.76
1	82.75	4.96	0.20	0.70
3	6.91	2.48	0.22	0.72
5	17.66	4.99	0.03	0.70
10	29.24	6.98	0.03	0.77
US processed prepared SPNE films				
0	343.29	59.60	0.03	0.77
1	29.54	2.04	0.53	0.71
3	63.06	4.68	0.05	0.80
5	53.08	6.16	0.09	0.74
10	23.67	2.66	0.15	0.75
US–MW processed prepared SPNE films				
0	52.61	5.82	0.08	0.80
1	58.77	16.00	0.07	0.81
3	145.90	16.60	0.07	0.81
5	59.36	2.92	0.10	0.82
10	41.04	6.06	0.05	0.82

(PMMA–PEO)–$LiClO_4$–x wt % MMT electrolyte films have the low frequency ε' values of the order of 10^1-10^2, which are much lower than the ε' values of PEO-based electrolytes. This behavior is expected because in the prepared blend electrolytes the PMMA amount is four times more as compared to that of the PEO.

Figure 3(a–c) shows that the ε'' values of these polymer blend-based electrolyte films at fixed frequency are in the same order as that of their corresponding ε' values i.e. the electrolyte film of high ε' value also has relatively high ε'' value, and vice-versa. Further, the ε'' spectrum of the electrolytes at each MMT concentration has either one inflexion point or a broad peak related to singular molecular dielectric relaxation process which is influenced by the sample preparation methods. The peaks are observed in the ε'' spectra for few samples only, which are corresponding to the most probable molecular reorientation relaxation time τ_ε. But for comparative study of the molecular dynamics (polymer segmental motion) in these electrolytes with variation of MMT concentration and the sample preparation methods, the value of each sample relaxation time is needed. Therefore, the loss tangent (tan δ) and electric modulus spectra of these SPNE materials were considered and analyzed in order to evaluate the relaxation times for the confirmation of the behavior of molecular dynamics and its correlation with ion transport mechanism.

The σ' and tan δ spectra of the SC, US and US–MW methods prepared (PMMA–PEO)–$LiClO_4$–x wt % MMT electrolytes are depicted in Figure 4(a–c). It is found that the σ' values of these electrolytes increase non-linearly with the increase of frequency on logarithmic scale. The large decrease of σ' values with decrease of frequency below 10 kHz of these electrolytes are due to EP effect, which commonly occurs in SPE materials.[7,10,19] To find out the values of dc ionic conductivity σ_{dc}, the high frequency σ' spectra of these electrolytes are fitted to conventional Jonscher's power law[67] $\sigma'(\omega) = \sigma_{dc} + A\omega^n$, where A is the pre-exponential factor and n is the fractional exponent ranging between 0 and 1. The evaluated values of σ_{dc} and n for these electrolytes are given in Table I. The n values are found in the range 0.70 to 0.82, which suggest that the ions transportation in the electrolytes takes place through hopping mechanism.[7,10,63,68] The variation in n values confirms that the hop of ion motion is also influenced by the sample preparation methods. Further, the n values of these PMMA–PEO blend-based electrolytes are also found consistent of the n values (0.74–0.83) of PEO–$LiClO_4$ electrolyte films.[10] Recently, it has been derived and experimentally established that the complex conductivity spectra over the entire frequency range for the ion conducting materials can be correctly represented by the generalized Jonscher's law (GJ'sL),[69,70] which involves the universality of all types of dielectric polarization of a heterogeneous material. It is interesting here to report that the GJ'sL[69,70] is verified using our experimental results on the complex conductivity and permittivity of the polymeric electrolyte materials.[28] The aim of the present paper is to determine the dc conductivity and the ion conduction behavior, and therefore the conventional Jonscher's law[67] is fitted to the high frequency experimental values of σ' spectra which cover only the frequency range of dc plateau and the dispersion of dc to ac ion transportation as shown by solid lines in Figure 4.[7,11,29]

Figure 4(a–c) shows that the tanδ spectra of these PMMA–PEO blend-based electrolytes prepared by different methods have single relaxation peak at all the MMT concentrations. Earlier, the broadband DRS measurements established that the pristine

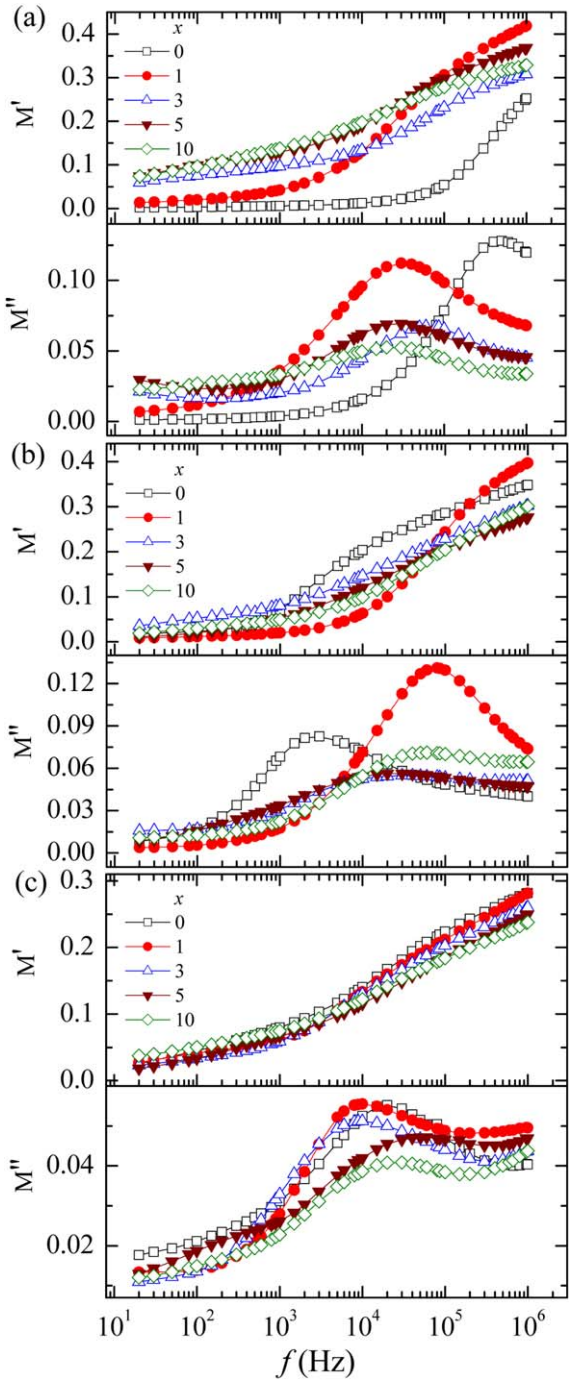

Figure 5. Frequency dependent real part M' and loss M'' of complex electric modulus of (PMMA–PEO)–$LiClO_4$–x wt % MMT nanocomposite electrolyte films prepared by (a) SC, (b) US, and (c) US–MW methods. [Color figure can be viewed in the online issue, which is available at wileyonlinelibrary.com.]

PMMA and PEO have multiple relaxation processes corresponding to their different dynamical phases.[71–76] Dielectric measurements on the frequency and temperature scale reveal that the amorphous PMMA has three relaxation processes corresponding to main chain segmental motion (cranckshaft or micro Brownian motion), the ester group rotation and the methyl group rotation, and they also merge to each other at different temperatures.[45,47,71,72] The recent study on the dielectric properties of PMMA/bentonite nanocomposite[76] also reported the tanδ peaks corresponding to the chain segmental dynamics of PMMA, which are found in agreement with the molecular dynamics of these PMMA–PEO blend electrolytes. The semicrystalline PEO has three main dielectric relaxation processes, which are associated with chain segmental motion separately in crystalline and noncrystalline phases, and the local twisting in the main chains of the amorphous phase.[73] But the observed single relaxation peak in the tan δ spectra of these polymers blend electrolytes at room temperature can be assigned to the coupled chains segmental dynamics in the amorphous phase of miscible PMMA–PEO blend. The values of dielectric loss tangent relaxation time $\tau_{\tan\delta}$ corresponding to the molecular segmental dynamics in the complex polymers blend electrolytes is determined using the relation $\tau_{\tan\delta} = 1/2\pi\ f_{p(\tan\delta)}$, where $f_{p(\tan\delta)}$ is the frequency of tanδ peak, and these values are given in Table I. The $\tau_{\tan\delta}$ values are of the order of $\sim 10^{-6}$ s, which are found nearly equal to that of the PEO–$LiClO_4$ electrolytes.[10] The recent study on PMMA–$LiClO_4$–x wt % MMT electrolytes have confirmed the fluctuating relaxation processes in these electrolytes with the variation of MMT concentration and the sample preparation methods.[5] The appearance of single relaxation peak in tanδ spectra of the PMMA–PEO blend-based electrolytes also confirms the miscible blend behavior of cooperative polymers dynamics in which the fluctuating relaxations of the PMMA are suppressed.

Figure 5(a–c) shows the electric modulus (real part M' and loss M'') spectra of the PMMA–PEO blend-based electrolyte films prepared through SC, US, and US–MW methods. These spectra are commonly plotted and analyzed for the solid dielectric materials, because they are free from the contribution of EP effect at low frequencies, and also independent of the type of electrodes material, the electrode/dielectric specimen contact and the adsorbed impurities in the sample.[5–7,28,29,63] It is observed that the shapes of the M' and M'' spectra of the studied SPNE films change with the sample preparation methods and the MMT concentration. At low frequency side of the spectra, the M' values are close to zero, whereas in the high frequency region they increase non-linearly with increasing frequency. Similar to the tan δ spectra, the sharp singular relaxation peak is appeared in the M'' spectrum of each electrolyte sample. But these peaks are found at higher frequency side as compared to the corresponding tan δ peaks. Using the M'' peak frequency values $f_{p(M'')}$, the electric modulus relaxation time τ_M of the electrolytes is determined by the relation $\tau_M = 1/2\pi f_{p(M'')}$, and the observed τ_M values are recorded in Table I. The τ_M is also referred as conductivity relaxation time τ_σ for the solid electrolyte materials, because in many cases it has direct correlation with the ionic conductivity which is governed by the cations coordinated polymer chain segmental dynamics.[3–7,10] Table I shows that the $\tau_{\tan\delta}$ value is higher than the corresponding τ_M value of the same composition material. It is expected because the τ_M is related with $\tau_{\tan\delta}$ by the relation $\tau_M = (\varepsilon_\infty/\varepsilon_s)\tau_{\tan\delta}$, where ε_s is the static permittivity and it is always greater than the ε_∞ value.

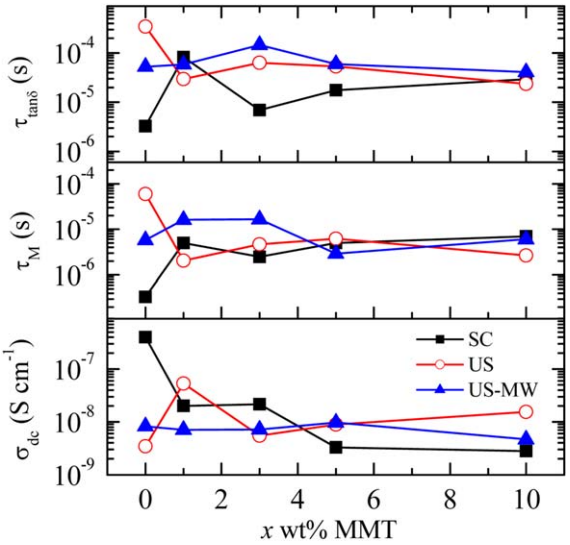

Figure 6. MMT concentration dependent loss tangent relaxation time $\tau_{tan\delta}$, electric modulus relaxation time τ_M and dc ionic conductivity σ_{dc} of (PMMA–PEO)–$LiClO_4$–x wt % MMT nanocomposite electrolyte films prepared by SC, US, and US–MW methods. [Color figure can be viewed in the online issue, which is available at wileyonlinelibrary.com.]

Figure 6 shows the variation of $\tau_{tan\delta}$, τ_M, and σ_{dc} values with MMT concentration of the (PMMA–PEO)–$LiClO_4$–x wt % MMT electrolytes prepared through different methods. It has been observed that the values of these parameters change anomalously with the increase of MMT concentration and also the electrolyte preparation methods. The anomalous variation of relaxation times with MMT concentration reveals that the cooperativity of PMMA and PEO chains dynamic is influenced by the amount of loaded MMT. The comparative values of relaxation times also infer that the dynamics of complex transient structures of the nanocomposite electrolytes vary with their preparation methods. These results are also favored by the structural properties of the electrolytes as revealed from their XRD measurements.

Before interpretation of σ_{dc} values of the (PMMA–PEO)–$LiClO_4$–x wt % MMT electrolytes, it is worthy here to report the conductivity behavior of individual polymer-based electrolytes. Recently,[7,10] authors studied the PEO–$LiClO_4$ electrolytes of varying salt concentrations [EO/Li^+ = 8, 12, 16, and 20] and prepared by SC, US, and US–MW methods. It was found that the σ_{dc} values of these electrolytes almost increase linearly from $\sim10^{-8}$ to 10^{-5} S cm^{-1} with the increase of salt concentration, at room temperature. Further, it was confirmed that the same method of sample preparation may not be always effective to increase the ionic conductivity of the electrolytes having different salt concentrations. Further, it was also revealed that in some cases the MMT nanofiller increases the σ_{dc} values of the PEO–$LiClO_4$–MMT electrolytes.[19,29] But the dispersion of organo-modified MMT mostly increases the σ_{dc} values of the PEO–$LiClO_4$ electrolytes[11] and also the PMMA–$LiClO_4$ electrolytes[21,25,35,36] by about 2 order of magnitude. At low salt concentrations, the σ_{dc} values of PEO–$LiClO_4$ and PMMA–$LiClO_4$ electrolytes are found of the order of $\sim10^{-9}$ to 10^{-7}, at room temperature, which may increase by two to three orders of magnitude with the addition of inorganic nanofillers and the liquid plasticizers.[11,21,25,32,34,39,77] Figure 6 shows that the σ_{dc} values of the (PMMA–PEO)–$LiClO_4$ electrolyte films of fixed salt concentration and without MMT vary by two orders of magnitude ($\sim10^{-7}$–10^{-9} S cm^{-1}) with the sample preparation methods. As compared to the σ_{dc} values of the US and US–MW processed prepared electrolyte films, the classical SC prepared electrolyte film has high σ_{dc} value. These σ_{dc} values of without MMT electrolyte films show a direct correlation with their relaxation time values. The high σ_{dc} value of the electrolyte film has low relaxation time, and vice versa. This observation reveals that the cations mobility is governed by the chain segmental dynamics of the polymers blend in these electrolyte films, which is in agreement with the conclusions drawn on the other solid polymeric electrolytes when they were investigated by the dielectric relaxation spectroscopy.[3,5–7,27–29,63] These studies revealed that the fast polymer chain dynamics (low relaxation time) increases the cations mobility, and hence there is increase of ionic conductivity of the solid polymeric electrolytes.[6,7,27–29] The observed σ_{dc} values of these polymer blend electrolytes of low salt concentration are also found of the order of their constituents polymer-based electrolytes of normal salt concentration. Recently,[55] the study on (PMMA–PEO)–$LiClO_4$ electrolyte having 80:20 wt % PMMA and PEO with 1 wt % $LiClO_4$ revealed its ambient temperature ionic conductivity value of 2.51×10^{-9} S cm^{-1}. This conductivity value is low as compared to the electrolytes investigated in the present study, which is expected because of very low salt concentration. Further, it has also been established that the polymer blend electrolyte of the equal amount of PMMA and PEO have the conductivity value $\sim10^{-8}$ S cm^{-1}.[22]

When only 1 wt % MMT is loaded in the polymeric blend electrolyte material, it significantly changes the relaxation times and the σ_{dc} values (Figure 6). A clear correlation is also found between the relaxation times and σ_{dc} values of the 1 wt % MMT filled polymer blend electrolyte films prepared through different processing methods. In case of SC prepared electrolyte film, the τ ($\tau_{tan\delta}$ and τ_M) values have an increase by more than one order of magnitude, which results a decrease of its σ_{dc} value by the same order. The increase of τ values suggest the increase in confinement effect on the polymer blend dynamics.[54,64] A relatively small increase in the τ values is observed for the US–MW prepared electrolyte film and therefore its σ_{dc} values shows a little decrease as compared to that of without MMT film (Figure 6). In case of US prepared electrolyte, the τ values have a decrease of about one order of magnitude and simultaneously the σ_{dc} increases by the same order. When the MMT concentration in these electrolytes increases above 1 wt %, the observed σ_{dc} values of the electrolyte films also have the correlation with their relaxation times. Figure 6 shows that there is less variations in the σ_{dc} values with increase of MMT concentration for the electrolyte films prepared through US–MW processing method. This result suggests the formation of some uniform structural properties in regards to the ion conduction paths when the films are prepared using US–MW processed solutions. This fact is also favored by the MMT concentration dependent

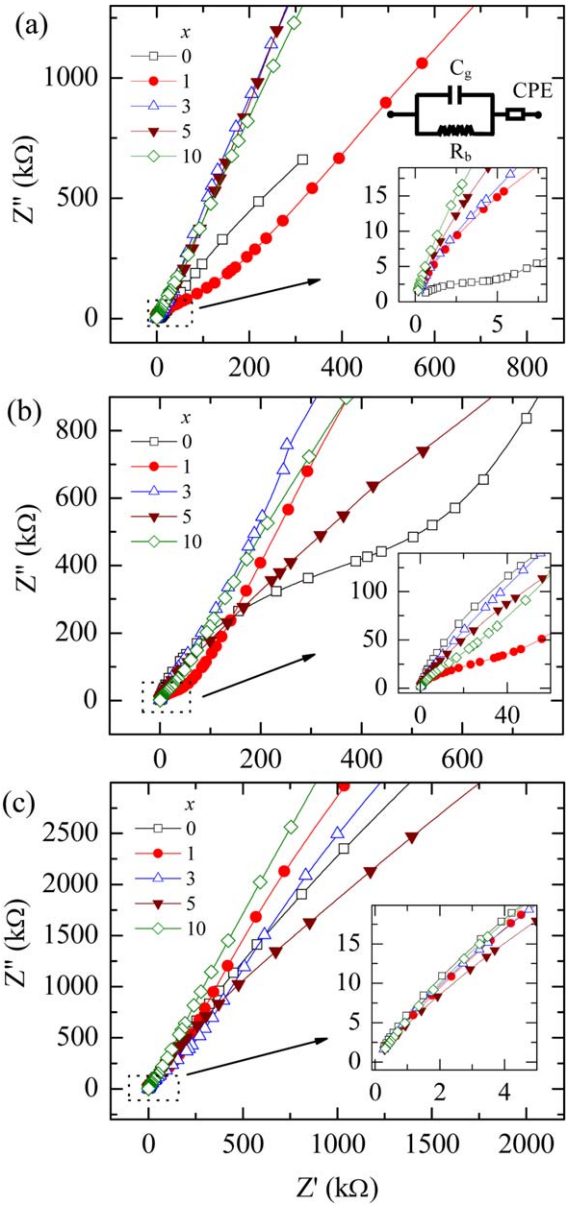

Figure 7. Complex impedance plane plots (Z'' *vs.* Z') of (PMMA–PEO)–$LiClO_4$–*x* wt % MMT nanocomposite electrolyte films prepared by (a) SC, (b) US, and (c) US–MW methods. [Color figure can be viewed in the online issue, which is available at wileyonlinelibrary.com.]

linear increase of the 001 peak intensity in the XRD patterns. Further, the σ_{dc} values of these electrolytes as determined by power law fit of the σ' spectra are found close to the earlier reported conductivity values of the (PMMA–PEO) blend-based nanocomposite electrolytes determined by the electrochemical impedance spectroscopy, at room temperature.[54,55] For these electrolytes of 80/20 wt % PMMA–PEO blend with 2 and 5 wt % MMT, their σ_{dc} values were 2.51×10^{-8} S cm^{-1} and 1×10^{-8} S cm^{-1}, respectively.[55]

The complex impedance plane plots (Z'' *vs.* Z') of the (PMMA–PEO)–$LiClO_4$–*x* wt % MMT electrolyte films prepared through SC, US, and US–MW methods are shown in Figure 7(a–c). Such plots are widely used for the electrochemical characterization of solid electrolyte materials.[5,9,11,22] These plots provide the information regarding the nature of charge carriers (electrons or ions), the frequency range over which the EP effect contribute in bulk properties and the behavior of electrode-electrolyte contact. Further, these plots are also used for the determination of dc ionic conductivity of the electrolytes. The polymeric electrolyte materials, those have contribution of electrode polarization phenomena in the bulk properties, result a spike in the low frequency region of their Z'' *vs.* Z' plot, whereas a semicircular type arc is appeared in the high frequency region corresponding to the bulk material properties.[9–11,20–22,26,35,78] The experimental data of the electrode/electrolyte/electrode cell of such electrolyte materials can be represented by an equivalent electrical circuit consisting a bulk resistance R_b in parallel with geometrical capacitance C_g and a constant phase element (CPE) in their series as depicted in the inset of Figure 7(a).[78] The significance of the frequency dependent total impedance of such equivalent circuit of a polymeric electrolyte material has been recently reported.[78] Further, the impedance values of these electrolytes at low frequencies are of several hundreds kΩ which decrease with increase of frequency and finally approach to very low values (few kΩ to hundreds of Ω) at 1 MHz.

The shapes of the complex impedance plane plots of the SC and US processed prepared electrolytes differ by a large amount with change of MMT concentration, whereas the US–MW processed prepared SPNE films have some symmetry in their plots. The arc type shapes of some of these plots at high frequencies [insets of Figure 7(a–c)] are due to bulk properties, and the inclined straight line behavior at low frequencies confirms the contribution of electrode polarization in the measured electrical properties of the electrolytes. The R_b value of the SPNE films can be obtained from common intercept of the semicircular arc and the straight line on the real axis of these impedance plots. Some plots of these electrolytes do not have arcs, which may be above the upper experimental frequency limit. The σ_{dc} values of such electrolytes can also be calculated by the relation $\sigma_{dc} = t_s/R_bA$, where t_s is the thickness and A is the surface area of the film.[5,11,22] In the present study, the σ_{dc} values of the SPNE films have been determined by power law fit to the high frequency σ' experimental data, because the n values obtained by the power law fit provide the information about the behavior of ion transportation mechanism, which is hopping type mechanism for these electrolytes as discussed above. However, there may be a small difference in the conductivity values of the electrolytes determined by power law fit of the σ' spectra and also from the R_b value obtained from the impedance plots.

CONCLUSIONS

The comparative dielectric properties, relaxation times, ionic conductivity, and the structural behavior of (PMMA–PEO)–$LiClO_4$–*x* wt % MMT nanocomposite electrolytes prepared by three different methods (SC, US, and US–MW) were reported. The variation of the dielectric parameters with the sample preparation methods and the MMT concentration were explored. The results of these PMMA–PEO blend-based electrolytes were compared with the dielectric and structural properties of their

individual polymer-based electrolytes. The ionic conductivity values of these electrolytes are governed by the conductivity relaxation times. The SC method has the advantage in regards to the enhancement of the ionic conductivity for the electrolyte film of without MMT, but in this method conductivity decreases anomalously with MMT concentration. The US–MW method verifies its suitability for maintaining almost same ionic conductivity over the entire MMT concentration range for the electrolytes. In these PMMA–PEO (80:20 wt %) blend-based electrolytes, the PEO has the total miscibility with PMMA domain due to which crystalline phase of the PEO is completely suppressed. The presence of single relaxation peak in the dielectric loss and electric modulus spectra of these electrolytes over the frequency range 20 Hz to 1 MHz confirms the cooperative molecular dynamics of the PMMA and PEO chains those have the coupling through lithium cation coordination. Due to PMMA–PEO chain dynamical cooperativity, the intercalated MMT structures are formed in these SPNE films which are influenced by the sample preparation methods. The structural symmetry is less influenced with the increase of MMT concentration when the electrolytes are prepared through US–MW processing method. In the PMMA–PEO blend-based electrolytes, the presence of low amount of PEO in the PMMA matrix mainly governs their structural and dielectric properties. The ionic conductivity values of these polymer blend electrolytes of low salt concentration are found of the order of their individual polymer-based electrolytes having normal salt concentration. The significant ionic conductivity values at room temperature of these low salt concentration electrolytes confirm their potential applications for the electrochromic devices, and also as the electrolyte material for lithium ion batteries. Further, the intercalated amorphous structures of the (PMMA–PEO)–$LiClO_4$–*x* wt % MMT electrolytes make them novel over the exfoliated amorphous PMMA–$LiClO_4$–*x* wt % MMT electrolytes and the intercalated semicrystalline PEO–$LiClO_4$–*x* wt % MMT electrolytes.

ACKNOWLEDGMENTS

Authors are grateful to the Department of Science and Technology (DST), New Delhi, for providing the experimental facilities through research projects Nos. SR/S2/CMP-09/2002 and SR/S2/CMP-0072/2010, and the DST–FIST program. One of the authors S.C. is thankful to the DST, New Delhi, for the award of SERB Fast Track Young Scientist research project No. SR/FTP/PS-013/2012.

REFERENCES

1. Chen, H. W.; Xu, H. Y.; Huang, C. F.; Chang, F. C. *J. Appl. Polym. Sci.* **2004**, *91*, 719.
2. Park, M. J.; Choi, I.; Hong, J.; Kim, O. *J. Appl. Polym. Sci.* **2013**, *129*, 2363.
3. Karan, N. K.; Pradhan, D. K.; Thomas, R.; Natesan, B.; Katiyar, R. S. *Solid State Ionics* **2008**, *179*, 689.
4. Zhou, X.; Yin, Y.; Wang, Z.; Zhou, J.; Huang, H.; Mansour, A. N.; Zaykoski, J. A.; Fedderly, J. J.; Balizer, E. *Solid State Ionics* **2011**, *196*, 18.
5. Sengwa, R. J.; Choudhary, S. *J. Phys. Chem. Solids* **2014**, *75*, 765.
6. Karmakar, A.; Ghosh, A. *Curr. Appl. Phys.* **2012**, *12*, 539.
7. Choudhary, S.; Sengwa, R. J. *Mater. Chem. Phys.* **2013**, *142*, 172.
8. Stephan, A. M.; Kumar, T. P.; Thomas, S.; Thomas, P.S.; Bongiovanni, R.; Nair, J. R.; Angulakshmi, N. *J. Appl. Polym. Sci.* **2012**, *124*, 3245.
9. Syzdek, J.; Armand, M.; Marcinek, M.; Zalewska, A.; Żukowska, G.; Wieczorek, W. *Electrochim. Acta* **2010**, *55*, 1314.
10. Sengwa, R. J.; Choudhary, S. *Indian J. Phys.* **2014**, *88*, 461.
11. Mohapatra, S. R.; Thakur, A. K.; Choudhary, R. N. P. *J. Power Sources* **2009**, *191*, 601.
12. Deka, M.; Kumar, A. *J. Solid State Electrochem.* **2013**, *17*, 977.
13. Kumar, Y.; Pandey, G. P.; Hashmi, S. A. *J. Phys. Chem. C* **2012**, *116*, 26118.
14. Choi, Y. S.; Bae, Y. C.; Sun, Y. K. *J. Appl. Polym. Sci.* **2005**, *98*, 2314.
15. Kumar, Y.; Hashmi, S. A.; Pandey, G. P. *Solid State Ionics* **2011**, *201*, 73.
16. Deka, M.; Kumar, A. *J. Power Sources* **2011**, *196*, 1358.
17. Ramesh, S.; Liew, C. W.; Ramesh, K. *J. Appl. Polym. Sci.* **2013**, *127*, 2380.
18. Ramesh, S.; Liew, C. W. *J. Non-Cryst. Solids* **2012**, *358*, 931.
19. Choudhary, S.; Bald, A.; Sengwa, R. J. *Indian J. Pure Appl. Phys.* **2013**, *51*, 769.
20. Shukla, N.; Thakur, A. K. *Ionics* **2009**, *15*, 357.
21. Shukla, N.; Thakur, A. K. *Solid State Ionics* **2010**, *181*, 921.
22. Ghelichi, M.; Qazvini, N. T.; Jafari, S. H.; Khonakdar, H. A.; Farajollahi, Y.; Scheffler, C. *J. Appl. Polym. Sci.* **2013**, *129*, 1868.
23. Samad, Y. A.; Asghar, A.; Lalia, B. S.; Hashaikeh, R. *J. Appl. Polym. Sci.* **2013**, *129*, 2998.
24. Johan, M. R.; Fen, L. B. *Ionics* **2010**, *16*, 335.
25. Chen, H. W.; Chang, F. C. *Polymer* **2001**, *42*, 9763.
26. Kim, S.; Hwang, E. J.; Jung, Y.; Han, M.; Park, S. J. *Colloids Surf. A* **2008**, *313*, 216.
27. Choudhary, S.; Sengwa, R. J. *Ionics* **2012**, *18*, 379.
28. Choudhary, S.; Sengwa, R. J. *Indian J. Pure Appl. Phys.* **2011**, *49*, 204.
29. Choudhary, S.; Sengwa, R. J. *Ionics* **2011**, *17*, 811.
30. Ren, S.; Chang, H.; He, L.; Dang, X.; Fang, Y.; Zhang, L.; Li, H.; Hu, Y., Lin, Y. *J. Appl. Polym. Sci.* **2013**, *129*, 1131.
31. Marzantowicz, M.; Dygas, J. R.; Krok, F.; Florjańczyk, Z.; Zygadło-Monikowska, E. *J. Non-Cryst. Solids* **2007**, *353*, 4467.
32. Money, B. K.; Hariharan, K.; Swenson, J. *Solid State Ionics* **2012**, *225*, 346.
33. Fahmi, E. M.; Ahmad, A.; Rahman, M. Y. A.; Hamzah, H. *J. Solid State Electrochem.* **2012**, *16*, 2487.

34. Zhang, J.; Huang, X.; Wei, H.; Fu, J.; Huang, Y.; Tang, X. *J. Appl. Electrochem.* **2010**, *40*, 1475.
35. Deka, M.; Kumar, A. *Electrochim. Acta* **2010**, *55*, 1836.
36. Meneghetti, P.; Qutubuddin, S.; Webber, A. *Electrochim. Acta* **2004**, *49*, 4923.
37. Ahmad, A.; Rahman, M. Y. A.; Su'ait, M. S. *J. Appl. Polym. Sci.* **2012**, *124*, 4222.
38. Ahmad, S.; Saxena, T. K.; Ahmad, S.; Agnihotry, S. A. *J. Power Sources* **2006**, *159*, 205.
39. Shanmukaraj, D.; Wang, G. X.; Murugan, R.; Liu, H. K. *J. Phys. Chem. Solids* **2008**, *69*, 243.
40. Rajendran, S.; Uma, T.; Mahalingam, T. *Eur. Polym. J.* **2000**, *36*, 2617.
41. Rajendran, S.; Mahendran, O.; Kannan, R. *J. Solid State Electrochem.* **2002**, *6*, 560.
42. Tan, S. M.; Johan, M. R. *Ionics* **2011**, *17*, 485.
43. Rajendran, S.; Bama, V. S.; Prabhu, M. R. *Ionics* **2010**, *16*, 27.
44. Sivakumar, M.; Subadevi, R.; Rajendran, S.; Wu, N. L.; Lee, J. Y. *Mater. Chem. Phys.* **2006**, *97*, 330.
45. Dionísio, M.; Fernandes, A. C.; Mano, J. F.; Correia, N. T.; Sousa, R. C. *Macromolecules* **2000**, *33*, 1002.
46. Ngai, K. L.; Roland, C. M. *Macromolecules* **2004**, *37*, 2817.
47. Jin, X.; Zhang, S.; Runt, J. *Macromolecules* **2004**, *37*, 8110.
48. Liu, J.; Sakai, V. G.; Maranas, J. K. *Macromolecules* **2006**, *39*, 2866.
49. Mpoukouvalas, K.; Floudas, G. *Macromolecules* **2008**, *41*, 1552.
50. Sakai, V. G.; Maranas, J. K.; Peral, I.; Copley, J. R. D. *Macromolecules* **2008**, *41*, 3701.
51. Chen, C.; Maranas, J. K. *Macromolecules* **2009**, *42*, 2795.
52. Shi, W.; Han, C. C. *Macromolecules* **2012**, *45*, 336.
53. Schwahn, D.; Pipich, V.; Richter, D. *Macromolecules* **2012**, *45*, 2035.
54. Jeddi, K.; Qazvini, N. T.; Jafari, S. H.; Khonakdar, H. A. *J. Polym. Sci. Part B: Polym. Phys.* **2010**, *48*, 2065.
55. Jeddi, K.; Qazvini, N. T.; Jafari, S. H.; Khonakdar, H. A.; Seyfi, J.; Reuter, U. *J. Polym. Sci. Part B: Polym. Phys.* **2011**, *49*, 318.
56. Strawhecker, K. E.; Manias, E. *Chem. Mater.* **2000**, *12*, 2943.
57. Elmahdy, M. M.; Chrissopoulou, K.; Afratis, A.; Floudas, G.; Anastasiadis, S. H. *Macromolecules* **2006**, *39*, 5170.
58. Miwa, Y.; Drews, A. R.; Schlick, S. *Macromolecules* **2008**, *41*, 4701.
59. Zhu, J.; Start, P.; Mauritz, K. A.; Wilkie, C. A. *Polym. Degrad. Stabil.* **2002**, *77*, 253.
60. Unnikrishnan, L.; Mohanty, S.; Nayak, S. K.; Ali, A. *Mater. Sci. Eng. A* **2011**, *528*, 3943.
61. Chang, K. C.; Chen, S. T.; Lin, H. F.; Lin, C. Y.; Huang, H. H.; Yeh, J. M.; Yu, Y. H. *Eur. Polym. J.* **2008**, *44*, 13.
62. Stefanescu, E. A.; Stefanescu, C.; Negulescu, I. I.; Daly, W. H. *Macromol. Chem. Phys.* **2008**, *209*, 2320.
63. Sengwa, R. J.; Sankhla, S.; Choudhary, S. *Ionics* **2010**, *16*, 697.
64. Sengwa, R. J.; Choudhary, S.; Sankhla, S. *Compos. Sci. Technol.* **2010**, *70*, 1621.
65. Choudhary, S.; Sengwa, R. J. *J. Appl. Polym. Sci.* **2014**, *131*, 39898.
66. Reinholdt, M. X.; Kirkpatrick, R. J.; Pinnavaia, T. J. *J. Phys. Chem. B* **2005**, *109*, 16296.
67. Jonscher, A. K. Dielectric Relaxation in Solids; Chelsea Dielectric Press: London, **1983**.
68. Dyre, J. C.; Schrøder, T. B. *Rev. Mod. Phys.* **2000**, *72*, 873.
69. Popov, I. I.; Nigmatullin, R. R.; Koroleva, E. Yu.; Nabereznov, A. A. *J. Non-Cryst. Solids* **2012**, *358*, 1.
70. Popov, I. I.; Nigmatullin, R. R.; Khamzin, A. A.; Lounev, I. V. *J. Appl. Phys.* **2012**, *112*, 094107.
71. Bergman, R.; Alvarez, F.; Alegria, A.; Colmenero, J. *J. Chem. Phys.* **1998**, *109*, 7546.
72. Seki, Y.; Kita, R.; Shinyashiki, N.; Yagihara, S.; Yoneyama, M. *AIP Conf. Proc.* **2013**, *8151*, 466.
73. Jin, X.; Zhang, S.; Runt, J. *Polymer* **2002**, *43*, 6247.
74. Sengwa, R. J.; Choudhary, S. *Bull. Mater. Sci.* **2012**, *35*, 19.
75. Choudhary, S.; Sengwa, R. J. *J. Appl. Polym. Sci.* **2012**, *124*, 4847.
76. Kaya, A. U.; Güner, S.; Esmer, K.; *J. Appl. Polym. Sci.* **2014**, *131*, 39907.
77. Masoud, E. M.; El-Bellihi, A. A.; Bayoumy, W. A.; Mousa, M. A. *J. Alloys Compounds* **2013**, *575*, 223.
78. Nath, A. K.; Kumar, A. *Electrochim. Acta* **2014**, *129*, 177.